Available online www.ejaet.com

European Journal of Advances in Engineering and Technology, 2019, 6(12):13-33

Research Article ISSN: 2394 - 658X

A Case Study on Numerical Modelling of Tsunamis in Peru and Northern Chile

M A Sarker

Technical Director, Royal Haskoning DHV, Rightwell House, Bretton, Peterborough PE3 8DW, United Kingdom

---

ABSTRACT

Royal HaskoningDHV (hereafter RHDHV) has set up a regional tsunami model covering most of Peru and the northern Chile a) to assess the tsunami risks in the region and b) to carry out numerical modelling of tsunami wave propagation to derive tsunami levels and currents required for designing marine structures and facilities. This paper describes the tsunami risk assessment, derivation of initial tsunami conditions and methodology of tsunami wave propagation modelling and run-up level calculations. The 2001 earthquake (approximate epicentre 16.2°S, 73.8°W) was used as the basis for deriving the 1 in 100 years and 1 in 1000 years earthquake parameters which were then used for generating the corresponding initial tsunami conditions. Sample results from the tsunami wave propagation modelling study and run-up level calculations are presented in this paper for illustration purposes. The model could be used to simulate any tsunami generated anywhere within the model domain. The methodology described in this paper for assessing and modelling tsunamis in Peru and the northern Chile could also be applied to simulate tsunamis at other sites around the world.

Key words: Numerical modelling, natural hazards, risk assessment, tsunami, seismic waves, tsunamigenic earthquakes, run-up, port development, Peru, Chile

---

1. INTRODUCTION

"Tsunami" is a Japanese word written with two Chinese characters. "Tsu" means "harbour/port" and "nami" means "wave" and therefore "tsunami" means "harbour/port wave" in Japanese. Tsunamis seem to appear suddenly and become very violent in shallow areas, attacking low-lying areas that are actively used and densely populated, such as port areas [1].

Tsunamis cause significant damage to sea ports, oil terminals & jetties, offshore exploratory drilling rigs and offshore oil extraction rigs. Significant loss of life, damage to properties, transportation facilities, ecosystems and marine structures and facilities occur due to tsunamis. Damage due to collision among boats, small ships or larger vessels is common during a tsunami. Tsunamis put lives and properties in coastal areas at greater risks. They cause flooding and submergence of low lying areas causing loss of life and property.

As reported in [2], the World Bank's estimated economic cost due to the 2011 tsunami was US$235 billion, making it the costliest natural disaster in world history. During the 2001 tsunami in southern Peru at least 74 people were killed, 2,687 were injured and 64 people were missing.

A large tidal hydrodynamic model is required to simulate tsunami on a region. Given the above risks, RHDHV has developed a regional tidal hydrodynamic model covering most of Peru and the northern Chile to investigate hazards from tsunamis.

Initially a seismic study was carried out to identify the most critical tsunamigenic earthquake affecting the region. Both 1 in 100 years and 1 in 1000 years return period conditions were considered in the study. The earthquake parameters from the 2001 tsunamigenic earthquake were used to generate the initial tsunami conditions by considering non-uniform slip (vertical displacement of seabed during an earthquake) distribution over the fault line. The "Tsunami" toolbox under the Delft DashBoard developed by Deltares [3] was used to generate the initial tsunami conditions and the MIKE21 Model developed by DHI [4] was used to simulate the tsunami propagation. Triangular flexible mesh (unstructured mesh of variable cell size) was used maintaining required variable resolution and smooth transition to obtain accuracy in model results. Run-up levels were calculated from the tsunami modelling results using the AMAZON Model [5]. Sample results from the modelling study are presented in this paper for illustration purposes only.

The model could be used to simulate any tsunami generated anywhere within the model domain. The methodology described in this paper for assessing and modelling tsunamis in Peru and the northern Chile could also be applied to

simulate tsunamis at other sites around the world.

2. DEFINITION, CAUSES AND TERMINOLOGIES OF TSUNAMI

A tsunami (also known as a seismic sea wave) is a series of water waves (similar to shallow water waves) in a water body caused by the abrupt displacement of a large volume of water initially resembling a rapidly rising tide.

Tsunami wave periods ranges from minutes to hours (typically 5 to 60 minutes) having their wavelength much longer than sea waves and can travel long distances across the oceans. Their behaviour are similar to shallow water waves (because their wave length is >> water depth) which means that the speed (v) is calculated as the square root of the product of the water depth (h) and the acceleration due to gravity (g) as below:

$$v = (gh)^{\frac{1}{2}}$$

Consequently, tsunamis travel very fast in the deep oceans. For example, if the water depth is 5000m, the speed will be more than 200m/s or about 800km/hour. Tsunamis are rare and coastal projects do not always take them into account. However, for major projects the risks should be assessed.

The definition of tsunami water level and wave height used in the study is illustrated in Figure 1. A tsunami wave height refers to the vertical distance from trough to peak of a tsunami wave. A tsunami level is referred to the level of the water column above the Mean Sea Level (MSL). Any tsunami level in this paper refers to a level above the MSL.

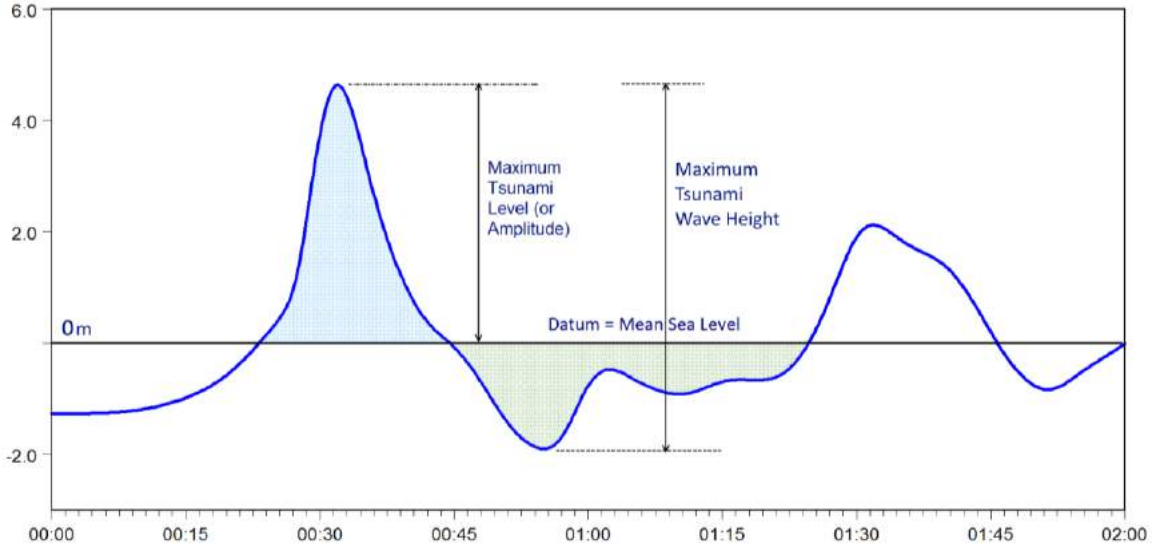

Fig.1 Definition of tsunami water level and tsunami wave height used in the study [18]

3. SOURCES OF TSUNAMIS AFFECTING THE REGION

A seismic risk assessment was carried out a) to identify the major fault lines in the region b) to assess the risks from tsunamis and c) to determine the most critical tsunamigenic earthquake affecting the region. Numerous published literatures and papers were obtained from public domain such as those by [6-11]. The seismic risk assessment suggests that the region is significantly affected by tsunamis.

The fault line is the so-called Peru-Chilean trench which is a result of a convergent boundary of the eastern edge of the oceanic Nazca Plate being sub-ducted beneath the continental South American Plate. In the region of interest, a seamount ridge within the Nazca Plate enters this subduction zone called the Nazca Ridge. Most of the tsunamigenic earthquakes that will be listed further occurred along this Peru-Chilean trench. Table 1 summarises the major tsunamigenic earthquakes in the study region of central/southern Peru.

Table -1 Summary of the major tsunamigenic earthquakes in the region

Date	Magnitude (M_w)	Approximate Epicenter	
		South Latitude	West Longitude
9 July, 1586	8.1	12.2°	77.7°
24 November, 1604	8.7	18.0°	71.5°
20 October, 1687	8.4	13.0°	77.5°
28 October, 1746	8.6	11.6°	77.5°
13 August, 1868	8.8	18.5°	71.2°
24 August, 1942	8.2	15.0°	76.0°
3 October, 1974	7.9	12.3°	77.8°
23 June, 2001	8.4	16.2°	73.8°
15 August, 2007	8.0	13.4°	76.5°

The 2001 earthquake occurred on 23/06/2001 20:33:15 with its epicentre at 16.20°S, 73.75°W. As this earthquake is

recent and its magnitude is relatively high, it was found to be critical for the study.

Data for tsunamigenic earthquakes and tsunami events from the Expert Tsunami Database for the Pacific (ETDB) and from the Tsunami Database of the National Geophysical Data Centre (NGDC) was used by [6] for long-term tsunami forecasting and for the determination of tsunami run-up distribution functions. The summary of the tsunami data is provided in Table 2 and the overview of the earthquake epicentres with M_w>6.0 for the coasts of Peru and Chile plotted on the basis of data from the ETDB Database (1471-2001) was shown in Kulikov et al. (2005). The overview of the tsunamigenic seismic events recorded on the coasts of Peru and Chile (a) from 1513 to 2001 and (b) from 1901 to 2001 on the basis of the ETDB Database was showed by [6]. The comparative analysis of [6] was extended using the data for the Pacific coast of South America from 5° to 35° South (adjacent to Peru and northern Chile). The calculated recurrence periods and tsunami heights from the corresponding data were compared with each other and with the estimations from other independent sources. Details of the ETDB/NGDC data and references are available from [6].

Table -2 Summary of tsunami data on the coasts of Peru and Chile (5°-35°S) from the NGDC and ETDB Databases [6]

Database	Period of observations (years)	Number of single tsunami observations	Number of tsunami events	
			Total	Applicable for analysis
NGDC	1562-2001	318	189	71
ETDB	1513-2001	270	139	92

4. RECURRENCE INTERVALS OF TSUNAMIGENIC EARTHQUAKES

The recurrence of tsunamigenic earthquakes on the coasts of Peru and Chile on the basis of the data (1) from 1513 to 2001 and (2) from 1900 to 2001 was presented by [6]. Their calculated values of the magnitudes M_s of tsunamigenic earthquakes for the given recurrence periods are provided in Table 3.

Silgado [12], as reported in [6], used the models of asymptotic limiting distributions of Gumbel of the first and third types to describe the distribution of the probability of the earthquake magnitudes. The estimates by [12] using the statistics for 1749–1974 are included into the table for comparison. It shows that the magnitudes obtained by [12] are smaller by 0.3–0.5 than those based on the ETDB data. This could be because of the fact that the statistics used by [12] were not sufficiently complete.

Table -3 Calculated values of the magnitudes of tsunamigenic earthquakes for the given recurrence periods [6]

Reference	Recurrence period (years)						
	2	5	10	20	50	100	200
ETDB (1513-2001)	5.88	7.46	7.96	8.28	8.55	8.68	8.78
Silagado (1749-1974)	-	-	-	-	8.04	8.35	8.47

Based on the above it was decided to adopt the return period values of the tsunamigenic earthquakes shown in Table 4 within the tsunami modelling for this study. These values are consistent with results from literature quoted above.

Table -4 Return period values of the tsunamigenic earthquakes used in the present study

Return periods (year)	Earthquake magnitude (M_w)
100	8.5
1000	8.9

5. EARTHQUAKE PARAMETERS

The 2001 earthquake was found to be critical for the study because it is a recent event and its magnitude is relatively high. Furthermore the 1 in 100 year earthquake magnitude of M_w 8.5 was close to the 2001 earthquake magnitude of M_w 8.4. Therefore, the 2001 earthquake basic parameters were adopted in the study. The summary of the earthquake parameters used in the study is provided in Table 5.

Although the magnitude of the 1 in 1000 year earthquake is higher than that of the 1 in 100 year earthquake, the general patterns of both earthquakes are similar. Therefore, the same basic parameters were used for both the 1 in 100 year and 1 in 1000 year earthquakes.

Table -5 Summary of the 2001 earthquake parameters used in the study

No.	Parameters	Values
1	Rupture time	23/06/2001 20:33:15
2	Type of thrust	Reverse
3	Latitude	16.2°S
4	Longitude	73.5°W
5	Magnitude (M_w)	8.4
6	Fault length	310 km
7	Fault depth	29 km
8	Dip angle	11/25° [average 18°]
9	Strike angle	310°

10	Slip angle (or rake angle)	70°

6. TSUNAMI MODELLING

6.1. The Tsunami Model

The MIKE21 Flow Model developed by DHI [4] was used to simulate the tsunamis. The regional model covers the coastlines of two countries – Peru and Northern Chile (see Figure 2). This regional tidal model was used to derive tsunami levels and currents in the study.

The use of powerful computers allowed the adoption of fine model mesh/grid to improve accuracy in simulation results. The higher order numerical scheme was used to improve accuracy in model prediction. Flooding and Drying were included in the model for treatment of the moving boundaries (flooding and drying fronts). Barotropic density and the Smagorinsky formulation for eddy viscosity were used in the model. Bed resistance was included in the model in the form of Manning's number. Varying Coriolis forces were applied to the model. A refined timestep of 15s was used in the model to obtain better accuracy in model prediction.

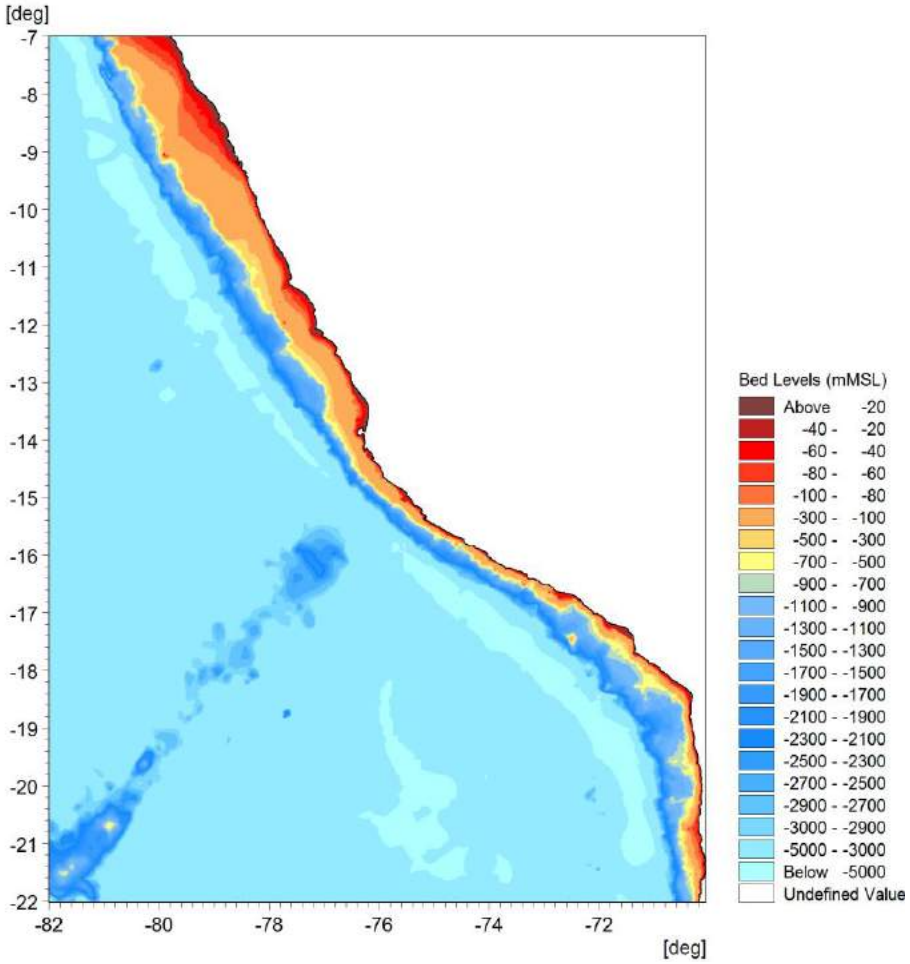

Fig. 2 Model domain and bathymetry

6.2. Tsunami Model Domain, Mesh and Bathymetry

Royal HaskoningDHV (RHDHV) has set up a regional tidal hydrodynamic model based on the MIKE21 Flow Model. The model covers the area from northern Peru to northern Chile as shown in Figure 2. This model was used to hindcast tsunamis in the study.

A flexible (triangular) mesh was used with variable mesh size distribution of required resolution and smooth transition to obtain accuracy in the model results. Particular attention was given to the fault line and the shallow areas. A smaller mesh size was also maintained in the areas where seabed slope is steep. Generally, 20-30 grids per wave length are recommended for simulating a tsunami, however, about 40 grids per wave length was used in the study to obtain higher accuracy in model results.

The mesh size distribution was generally as below:

- 50m grid size at 1m water depth
- 150m grid size at 10m water depth
- 500m grid size at 100m water depth
- 1500m grid size at ≥1000m water depth

The bathymetry of the wider domain was obtained from the C-Map Database [13]. Figure 2 shows the model bathymetry with respect to the Mean Sea Level (MSL) datum.

6.3. Tsunami Model Parameters

A constant water level equal to the Highest Astronomical Tide (HAT, +1.06m above the MLWS) was maintained over the entire model domain. The datum of the study was MSL (+0.39m above the MLWS). Mean Low Water Spring (MLWS) is 0.0m.

Some other major model parameters are given below:

- Time step = 15s;
- Run duration = 3 hours;
- Higher order numerical scheme used; and
- Coriolis force = varying in domain.

6.4. Tsunami Modelling Run Scenarios

A total of two runs were carried out as shown in Table 6.

Table -6 Tsunami modelling run scenarios

Runs	Earthquake magnitude (M_w)	Return periods (year)
1	**8.50**	**100**
2	**8.90**	**1000**

6.5. Chosen Location of Earthquake Epicentre

The earthquake return period investigations are not directly related to the earthquake location. There is equal chance that an earthquake of given magnitude might occur anywhere along the fault line. The earthquake sources applied in this study were assumed to be located in front of a chosen location as shown in Figures 3 and 4. In reality the earthquake may occur at anywhere along the fault line.

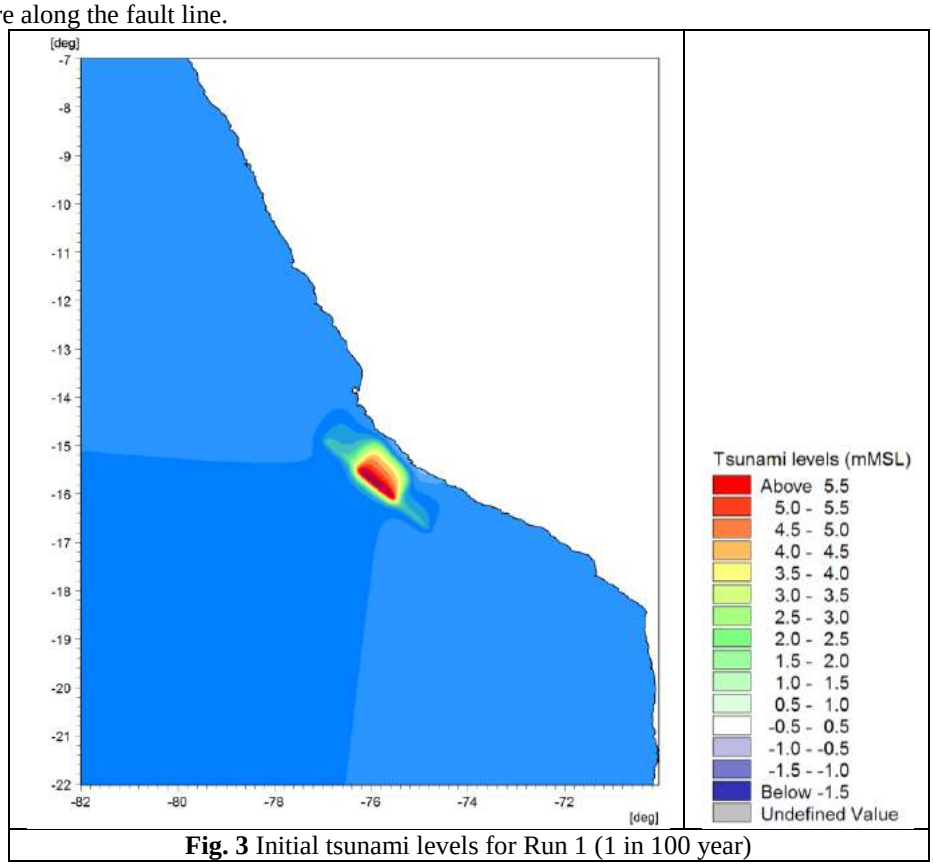

Fig. 3 Initial tsunami levels for Run 1 (1 in 100 year)

6.6. Slip Distribution over the Fault Length

Non-uniform slips (vertical displacement of seabed during an earthquake) were used in the study to provide higher slip in the middle of the fault length and lower slips at its either sides which represents more realistic slip distribution over the fault length. The lengths of the segments were decided through trial and error method by keeping the earthquake magnitude unchanged. The entire fault length was divided into three segments for the 1 in 100 years condition and into five segments for the 1 in 1000 years condition.

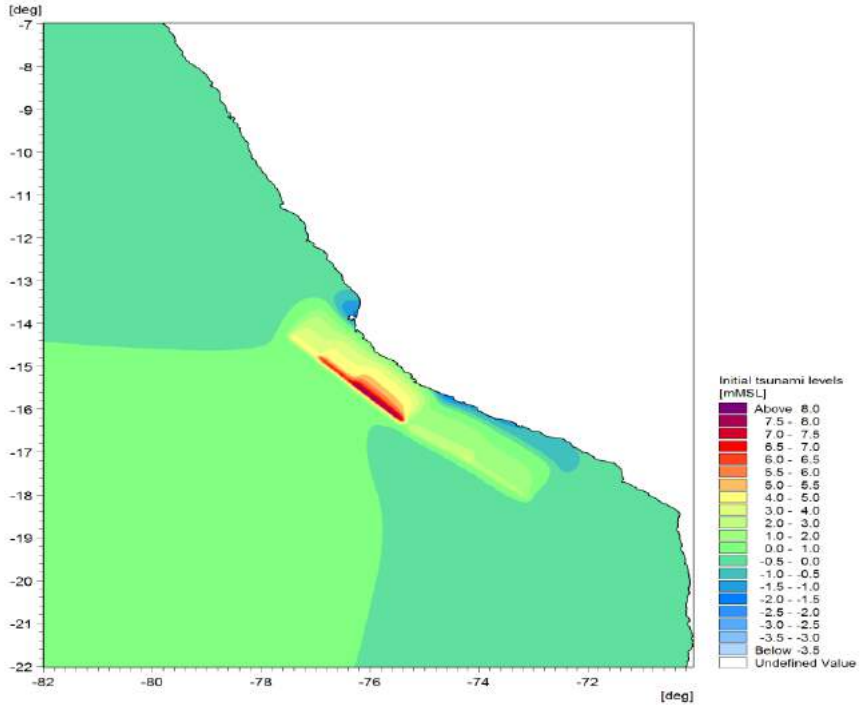

Fig. 4 Initial tsunami levels for Run 2 (1 in 1000 year)

6.7. Initial Tsunami Levels

The initial rise in the mean sea level due to the 1 in 100 year and 1 in 1000 year earthquakes was generated using the Tsunami Generation Tool of the Delft DashBoard developed by Deltares [3]. The Tsunami Generation Tool of the Delft DashBoard uses the [14] equation to calculate the surface deformation due to shear and tensile faults. The earthquake parameters described earlier in Table 5 were used in the tsunami generation tool. The maximum rise in the initial sea level for the two run scenarios are summarised in Table 7. The initial tsunami levels are illustrated in Figures 3 and 4.

Table -7 Maximum initial tsunami levels (+mMSL)

Runs	Earthquake magnitude (M_w)	Return periods (year)	Maximum initial tsunami levels (+mMSL)
1	8.50	100	5.8
2	8.90	1000	8.6

6.8. Tsunami Model Validation

The MIKE21 Flow Model is widely used for tsunami modelling worldwide, for example by [15-17].

The MIKE21 Flow Model was also used previously by Royal HaskoningDHV successfully for their project work to simulate the tsunami generated in the Makran Fault Line (along the Iranian and Pakistani coastlines) in 1945 to derive tsunami levels along the Omani coastline. The model results from Royal HaskoningDHV were compared to measured and numerically computed tsunami levels obtained from numerous published sources and an acceptable match was found. The tsunami model validation by Royal HaskoningDHV using the MIKE21 Flow Model is available in [18].

The overview of maximum tsunami level recorded on the coasts of Peru and Chile from 1575 to 2001 was presented by [6] on the basis of the ETDB Database. A tsunami level of about 9m was found for 2001.

The distribution of the maximum tsunami levels recorded on the coasts of Peru and northern Chile from 1575 to 2001 was presented by [6] on the basis of the ETDB Database. A tsunami level of about 8.5m was found near Pisco (north of the study site) and a tsunami level of about 9m was found at south of the study site (north of Matarani).

The relationship between the maximum tsunami level on the coasts of Peru and northern Chile and the tsunamigenic earthquake magnitudes was presented by [6]. Based on their relationship, a tsunami level of 9.6m was estimated on the coasts of Peru and northern Chile for the earthquake magnitude of 8.5 from the Silgado data.

Tsunami levels were extracted at the site from the present study. A maximum tsunami level of 9.8m was found at the site from the present study which compares well with the recorded data presented by [6].

The two-dimensional output of maximum tsunami level from the model is shown in Figure 5. The maximum tsunami level between Pisco and Camana is found between 6.0m and 8.0m (exceptions between 8-10m locally). This value is more or less is the same as values that were observed historically (i.e. 9m), if the same scenario is applied to these areas.

Few historical events were reported with the computed tsunami levels because it is suspected that there were few (if any) villages / cities existing between Pisco and Camana (distance ~490km). In both cities historical records have shown that tsunami level of ~9m have occurred in the past.

Photographs of damages caused by the 2001 earthquake were presented by [7]. The tsunami was described as

"destructive" that killed ~80 people. The inland flooding and run-up caused by the tsunami suggest that the tsunami level and the run-up level were very high.

It should be noted that tsunami levels intensify in bays, harbours and river mouths [6].

Based on the data presented above, a good overall agreement was found both in the pattern and the magnitude of maximum tsunami levels between Pisco and Camana reported by [6] and the results presented in the following section of this paper. Therefore, it is concluded that the present model is capable of predicting the tsunami levels at the study site with a good level of confidence.

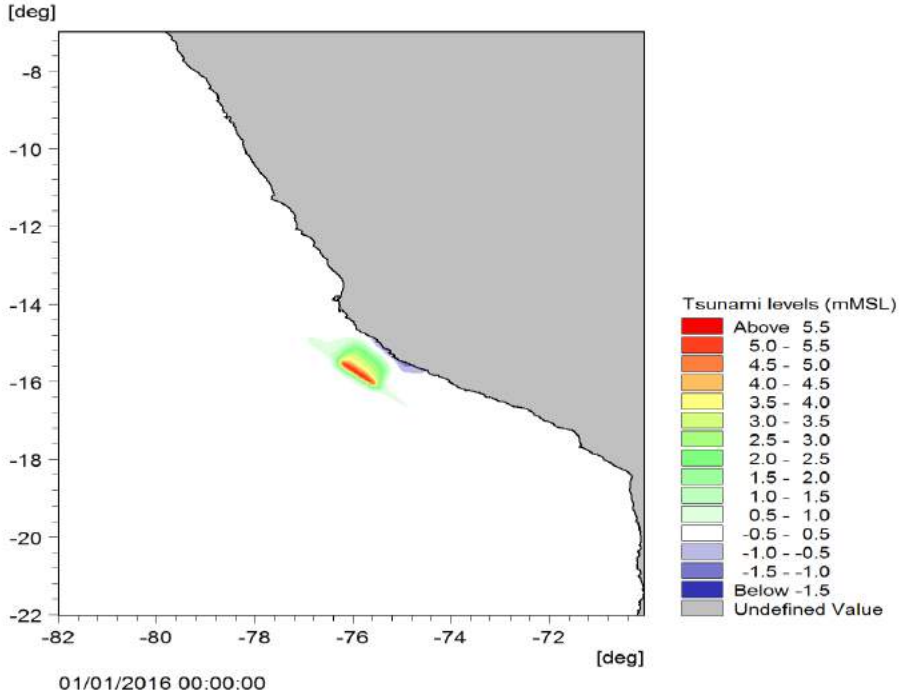

Fig. 5(a) Initial tsunami levels (t = 0)

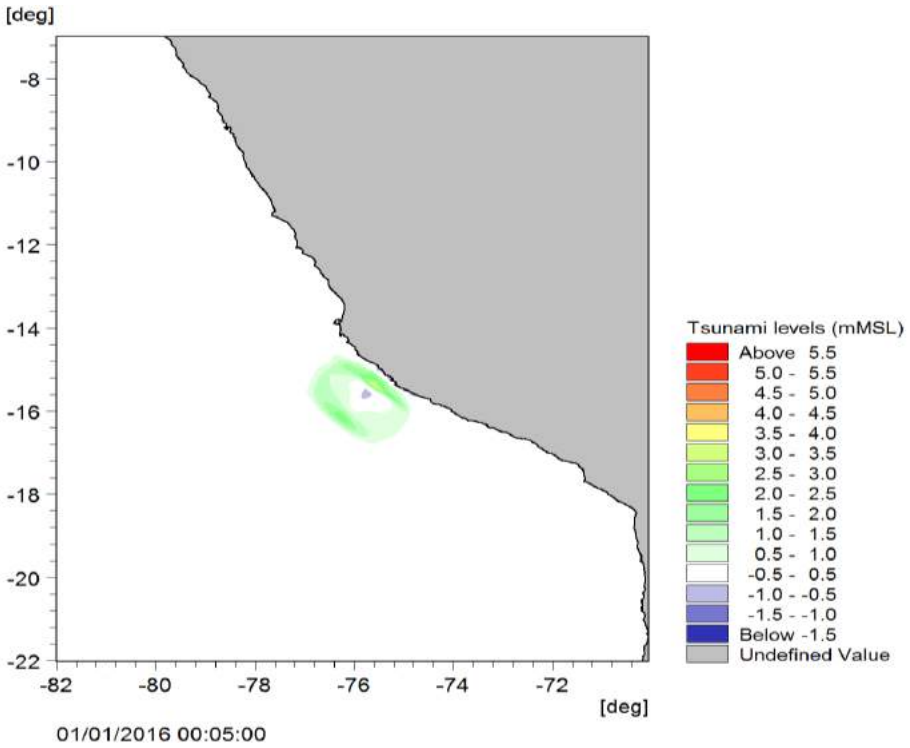

Fig. 5(b) Tsunami levels after 5 minutes

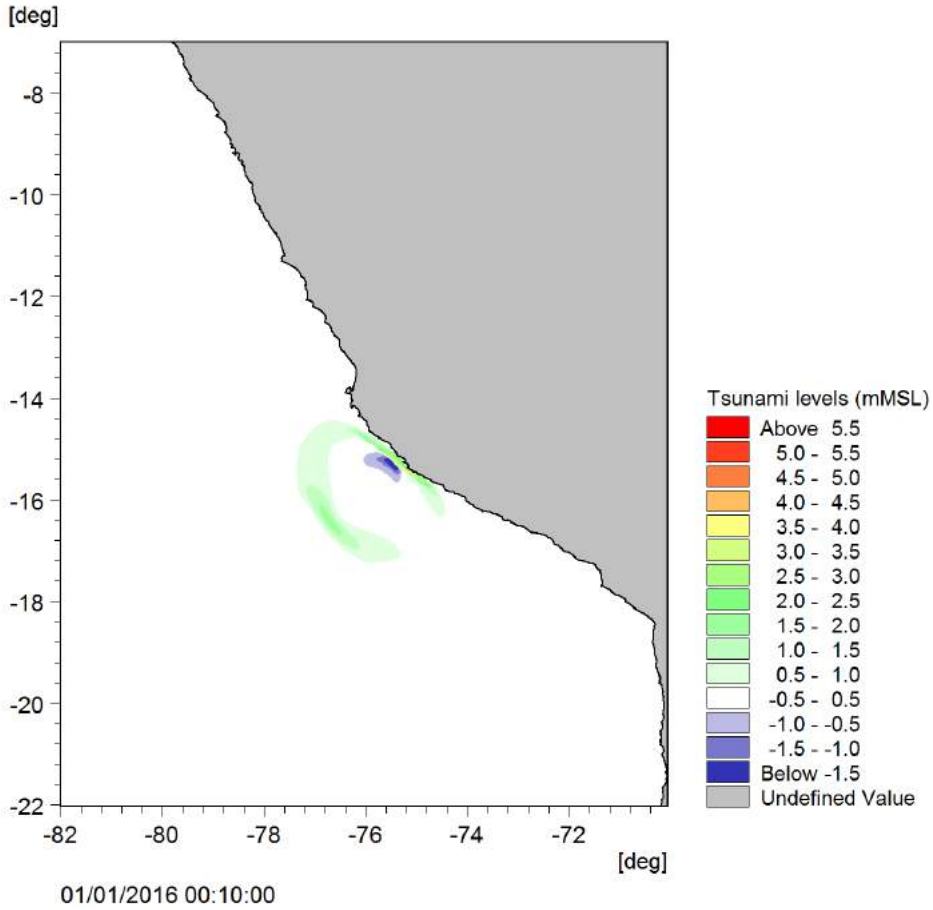

Fig. 5(c) Tsunami levels after 10 minutes

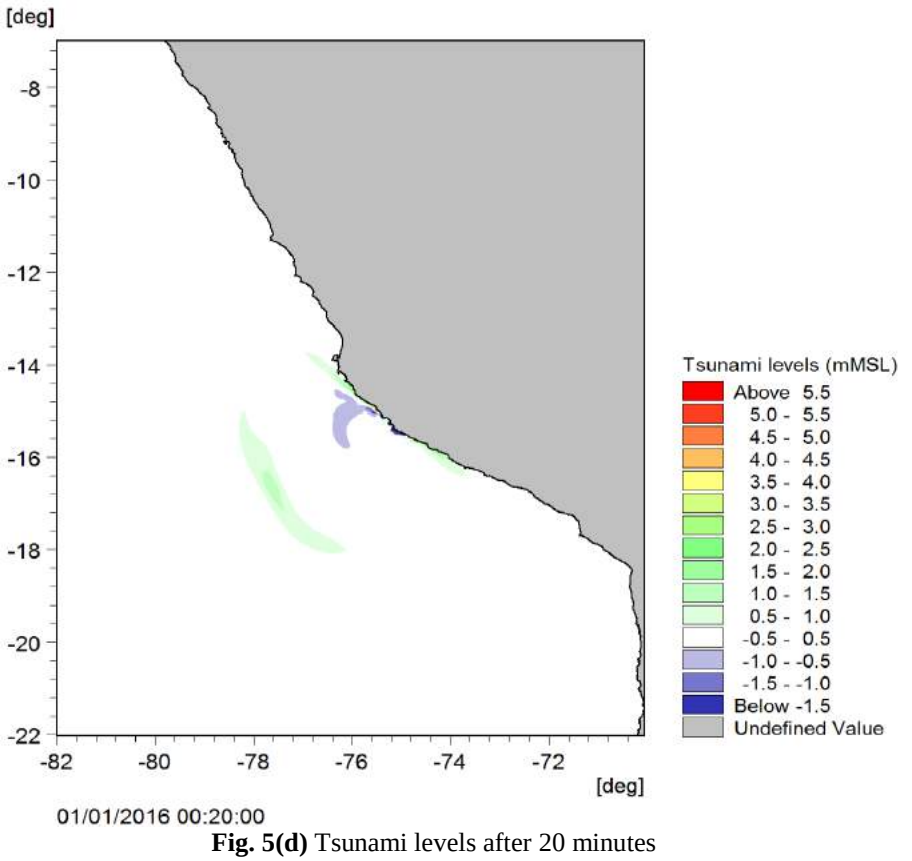

Fig. 5(d) Tsunami levels after 20 minutes

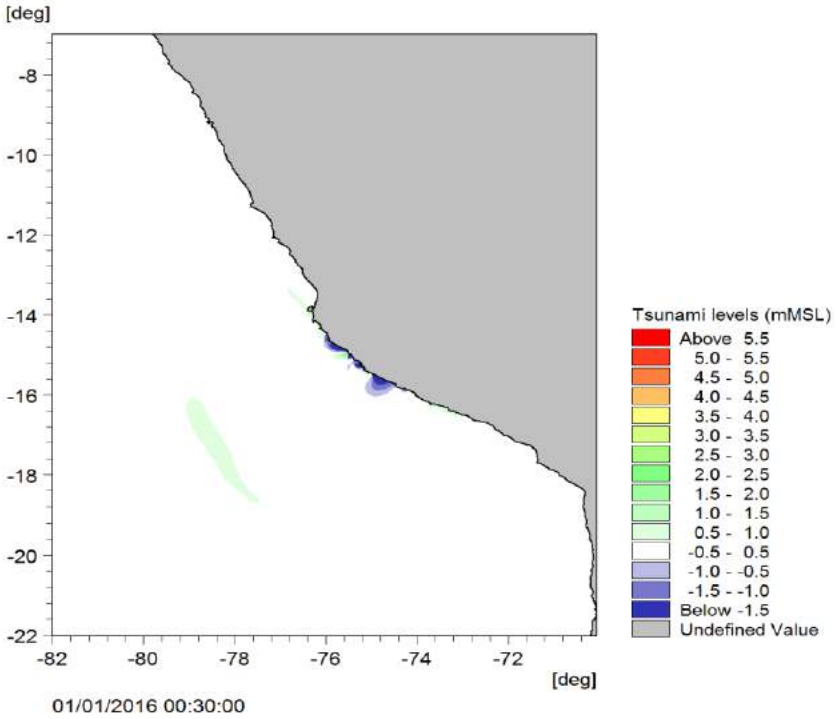

Fig. 5(e) Tsunami levels after 30 minutes

Fig. 5 Tsunami wave propagation over time for Run 1 (1 in 100 years)

6.9. Tsunami Model Results

6.9.1. Tsunami wave propagation over time

The propagation of tsunami waves over time (at time t = 0, 5, 10, 20 and 30 minutes) was extracted from model results. Figures 5(a) to 5(e) show the tsunami levels after 0, 5, 10, 20 and 30 minutes for Run 1 (1 in 100 years). Figures 6(a) to 6(e) show the tsunami levels after 0, 5, 10, 20 and 30 minutes for Run 2 (1 in 1000 years). The simulations indicate that it will take about 18 minutes for a tsunami to reach the coast.

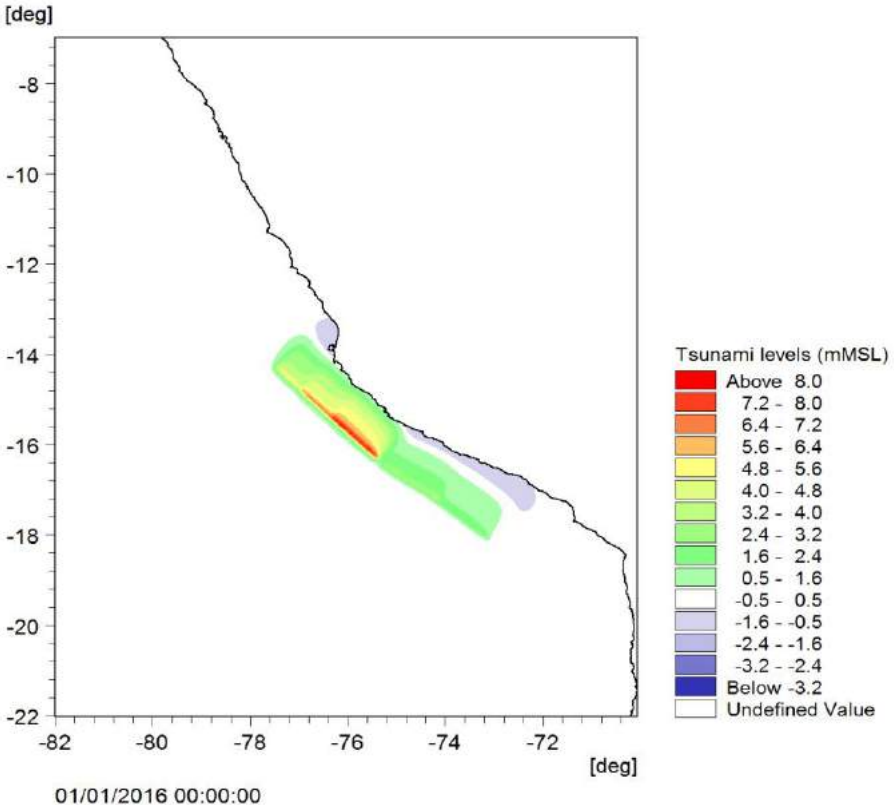

Fig. 6(a) Initial tsunami levels (t = 0)

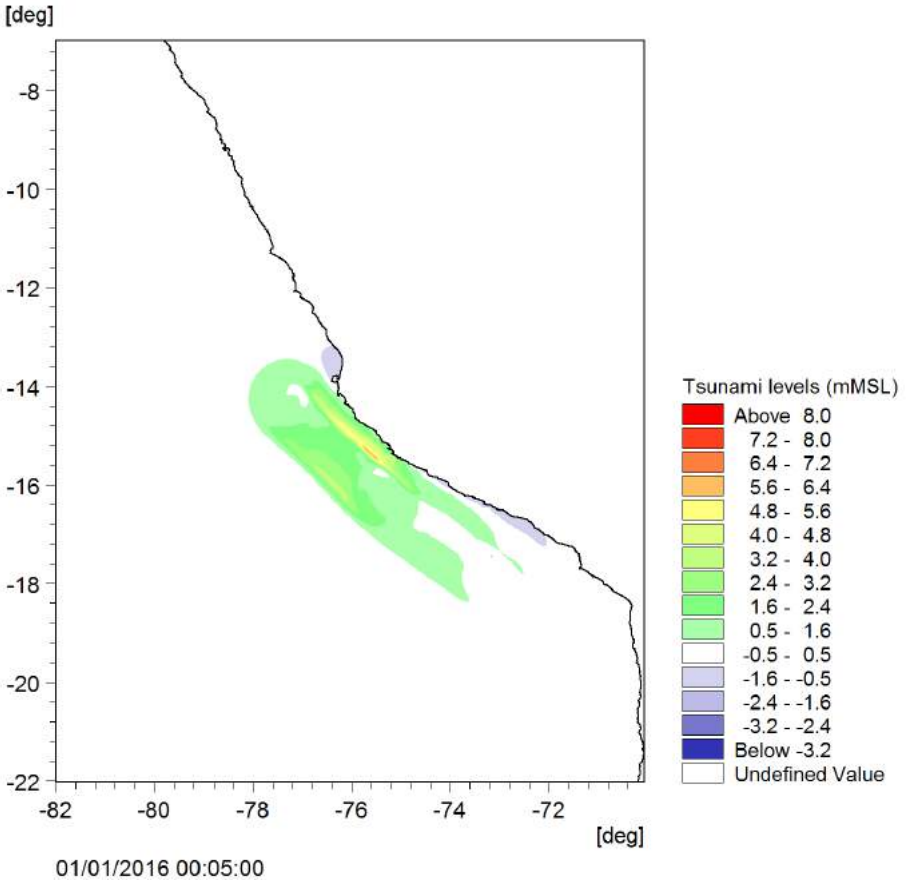

Fig. 6(b) Tsunami levels after 5 minutes

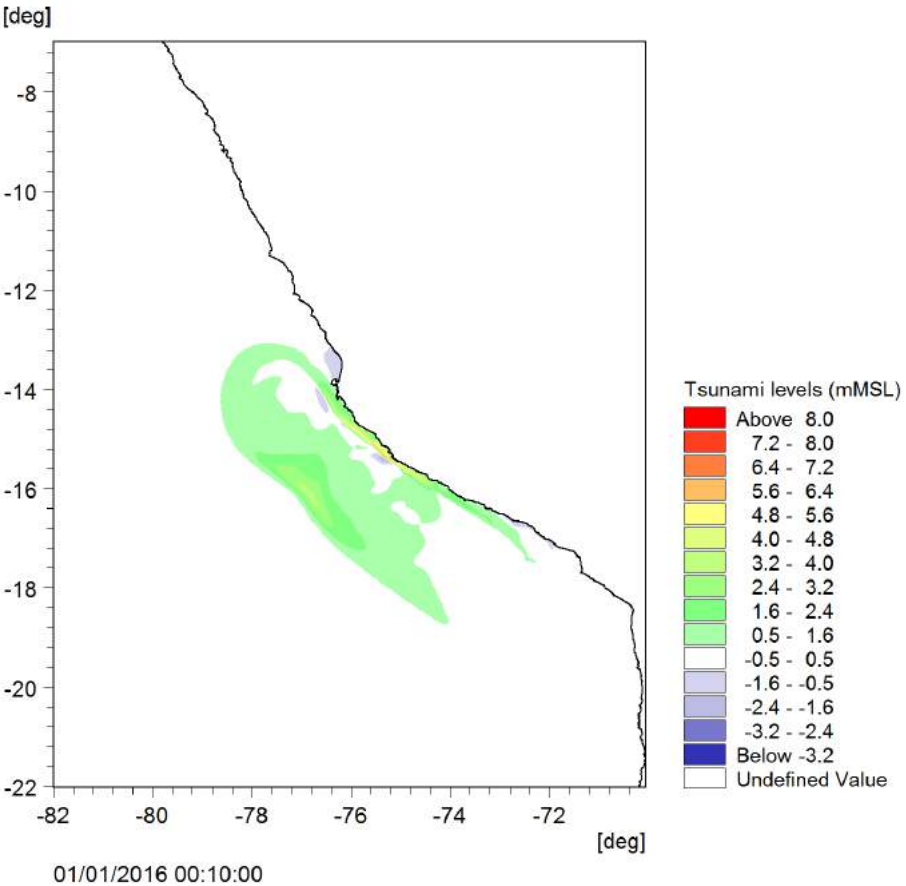

Fig. 6(c) Tsunami levels after 10 minutes

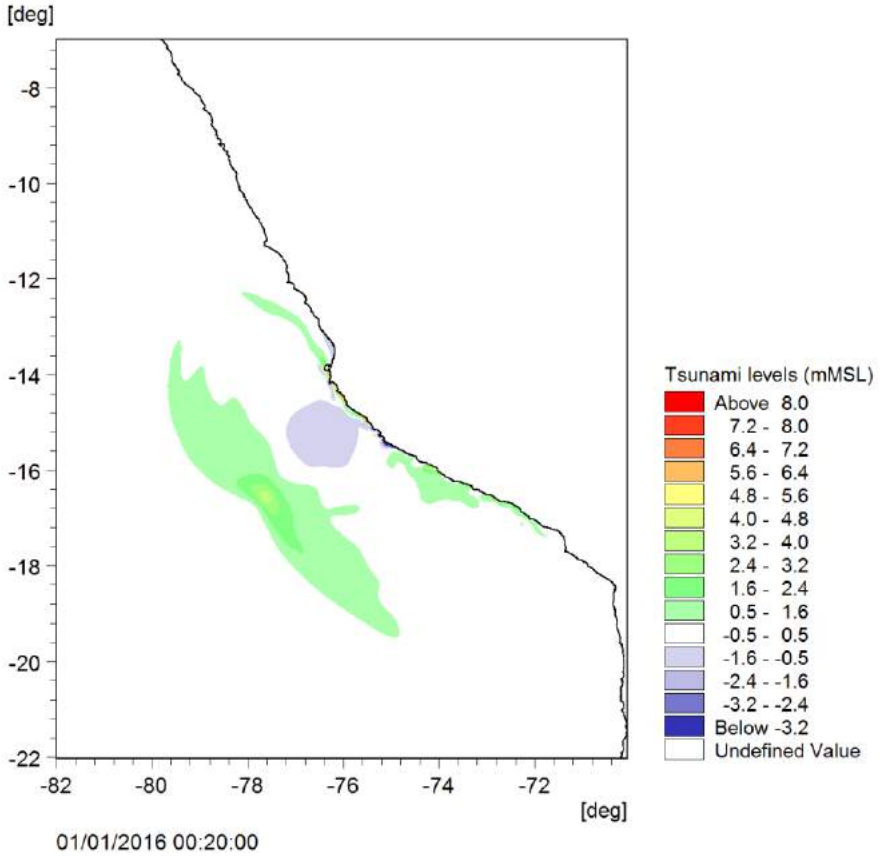

Fig. 6(d) Tsunami levels after 20 minutes

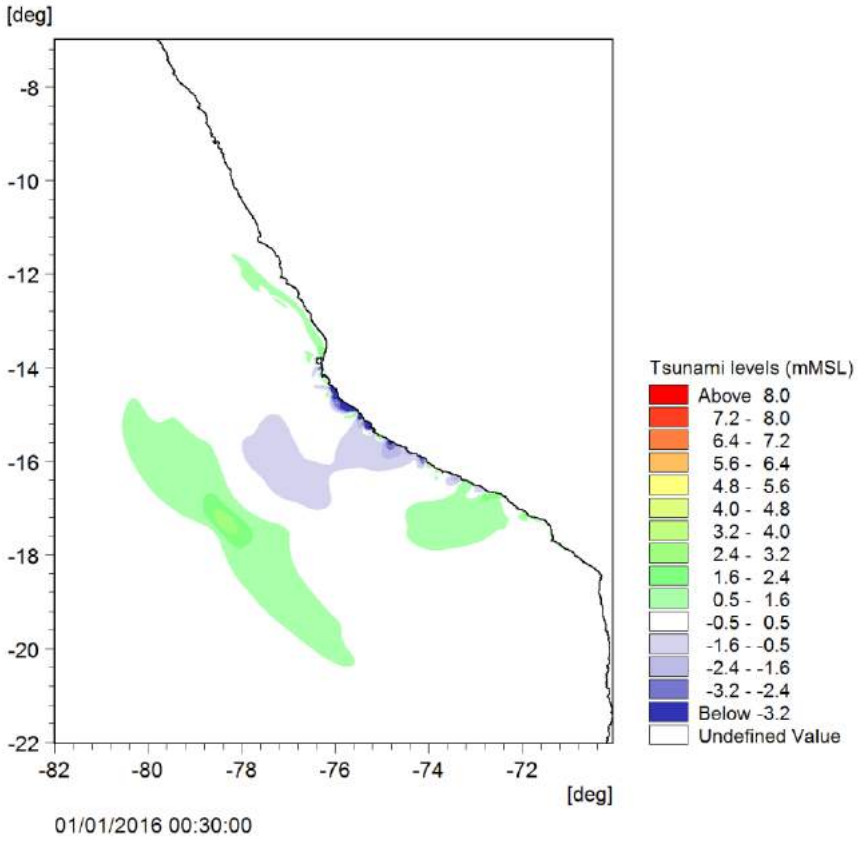

Fig. 6(e) Tsunami levels after 30 minutes

Fig. 6 Tsunami wave propagation over time for Run 2 (1 in 1000 year)

6.9.2. Two-dimensional output of maximum tsunami levels

Two dimensional plots of maximum tsunami levels during the entire 3 hours model simulation were generated from model results covering the entire domain. Figure 7 illustrates the maximum tsunami levels for Run 1 (1 in 100 years) and Figure 8 illustrates the maximum tsunami levels for Run 2 (1 in 1000 year). The figures suggest that the site is significantly affected by the tsunamis.

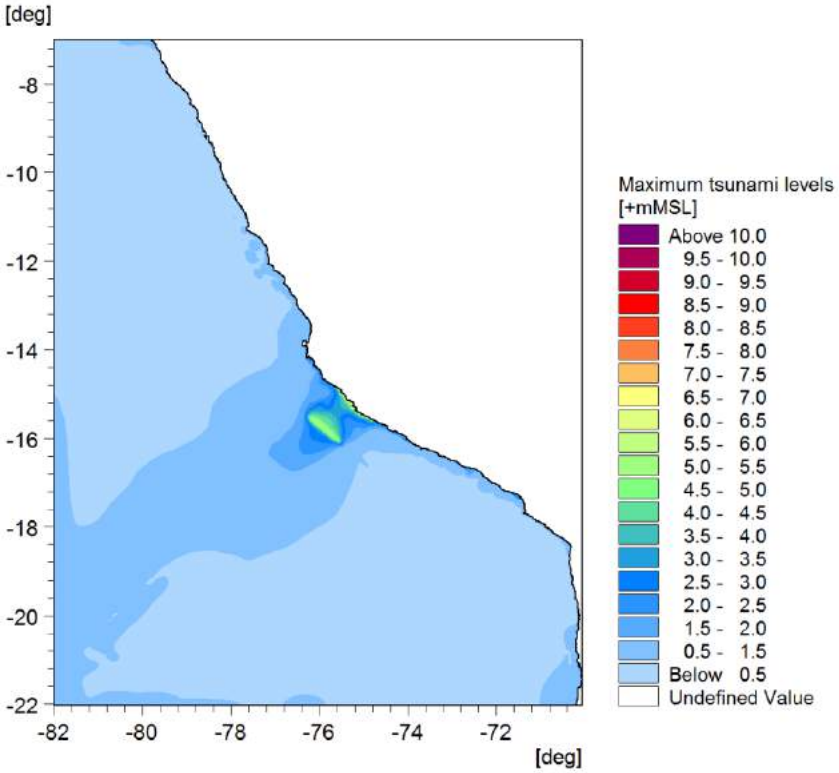

Fig. 7 Maximum tsunami levels during the entire 3 hours model simulation for Run 1 (1 in 100 years)

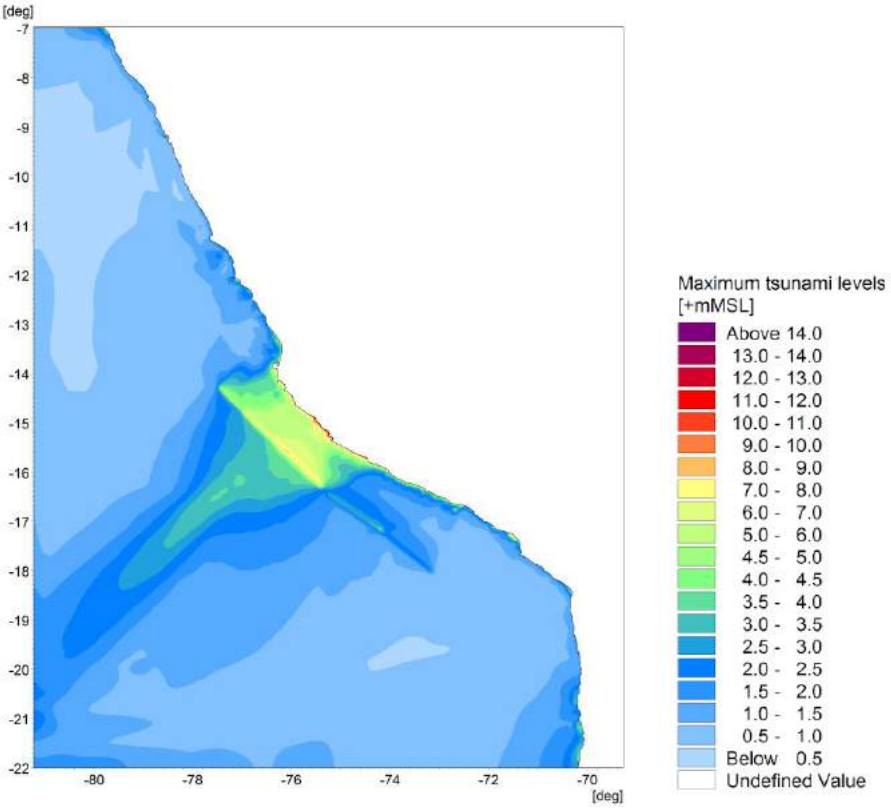

Fig. 8 Maximum tsunami levels during the entire 3 hours model simulation for Run 2 (1 in 1000 year)

6.9.3. Output of tsunami levels at selected water depths

Tsunami levels were extracted at various water depths. Figures 9(a) to 9(i) show the tsunami levels at -1, -3, -5, -12, -16, -21, -25, -50 and -100mMSL seabed levels for both 1 in 100 years and 1 in 1000 years conditions. Figures 10 and 11 show the tsunami levels at -1, -5, -25, 50 and -100mMSL seabed levels for Run 1 (1 in 100 year) and Run 2 (1 in 1000 year) respectively. Higher tsunami levels were found at shallower depths, as expected.

It should be noted that lines for the shallower water depths in Figures 10 and 11 are not continuous because this section of the bathymetry was subjected to drying during the trough phase of the wave.

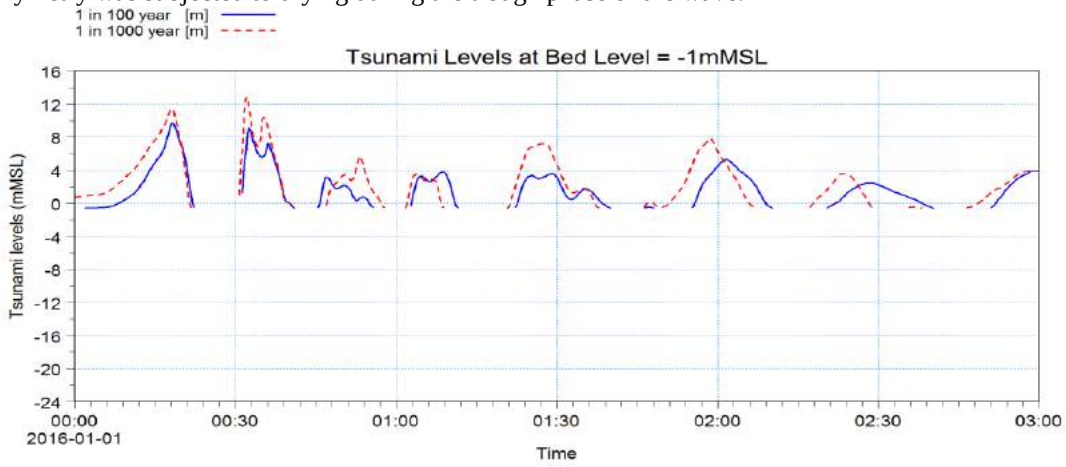

Fig. 9(a) Tsunami levels at seabed level of -1mMSL

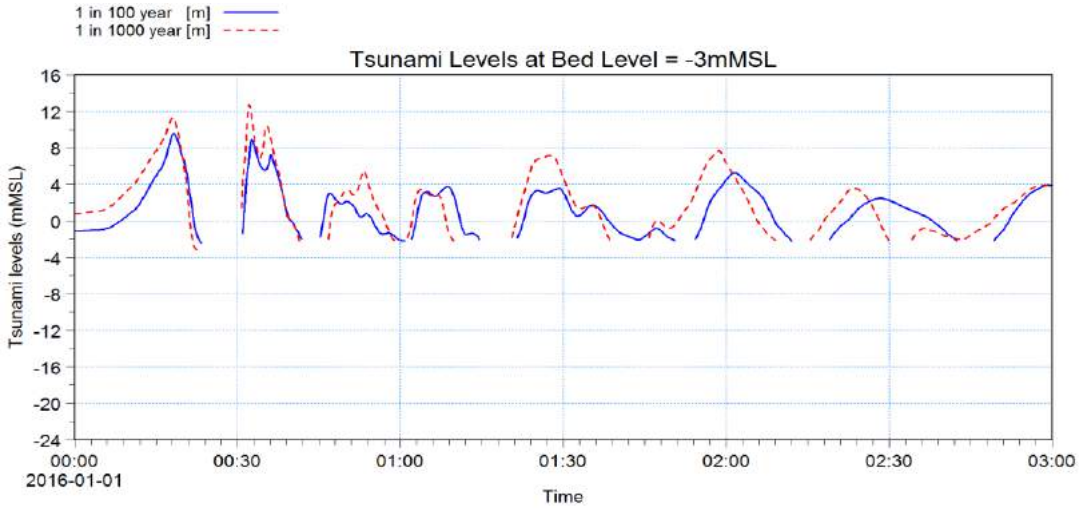

Fig. 9(b) Tsunami levels at seabed level of -3mMSL

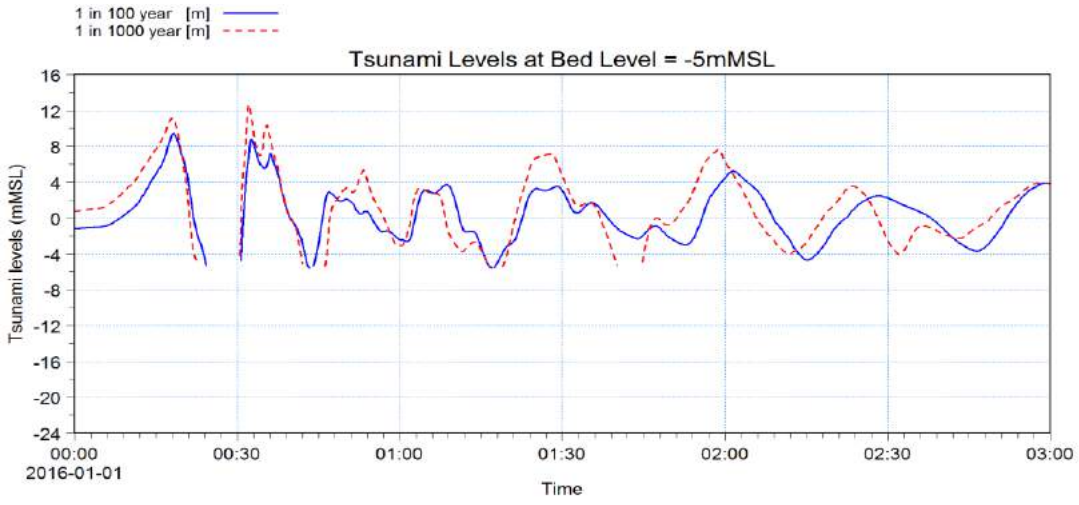

Fig. 9(c) Tsunami levels at seabed level of -5mMSL

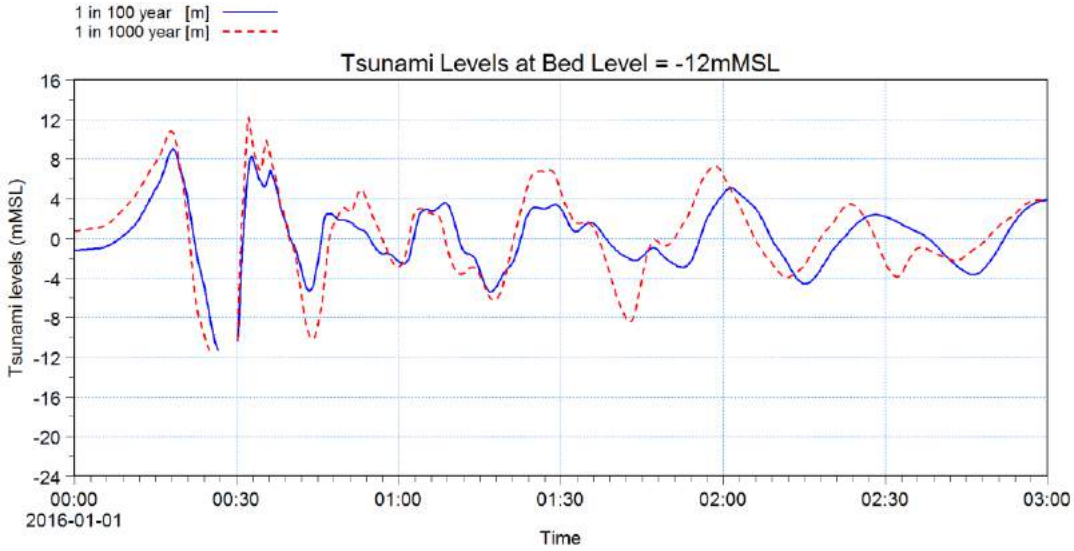

Fig. 9(d) Tsunami levels at seabed level of -12mMSL

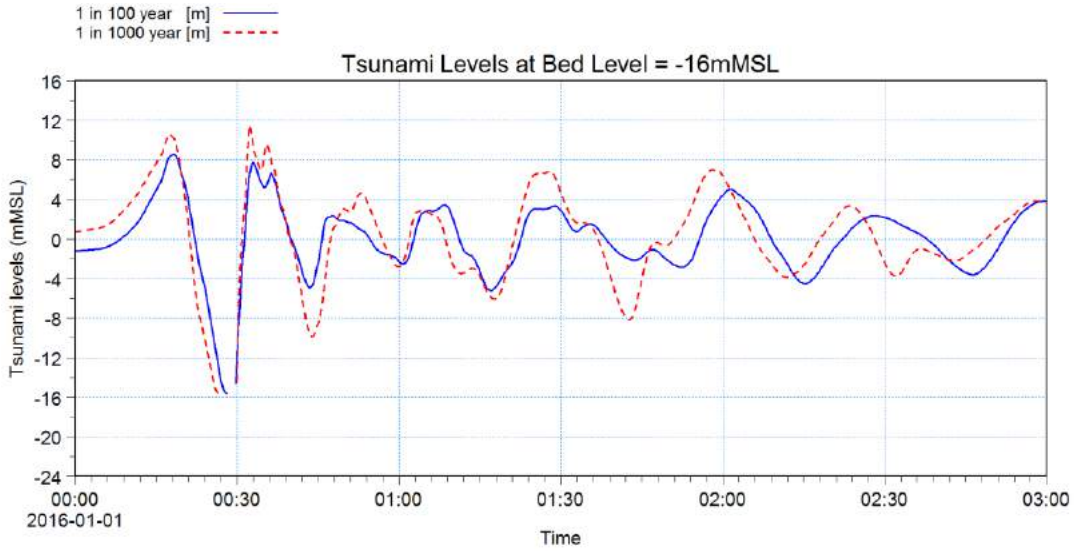

Fig. 9(e) Tsunami levels at seabed level of -16mMSL

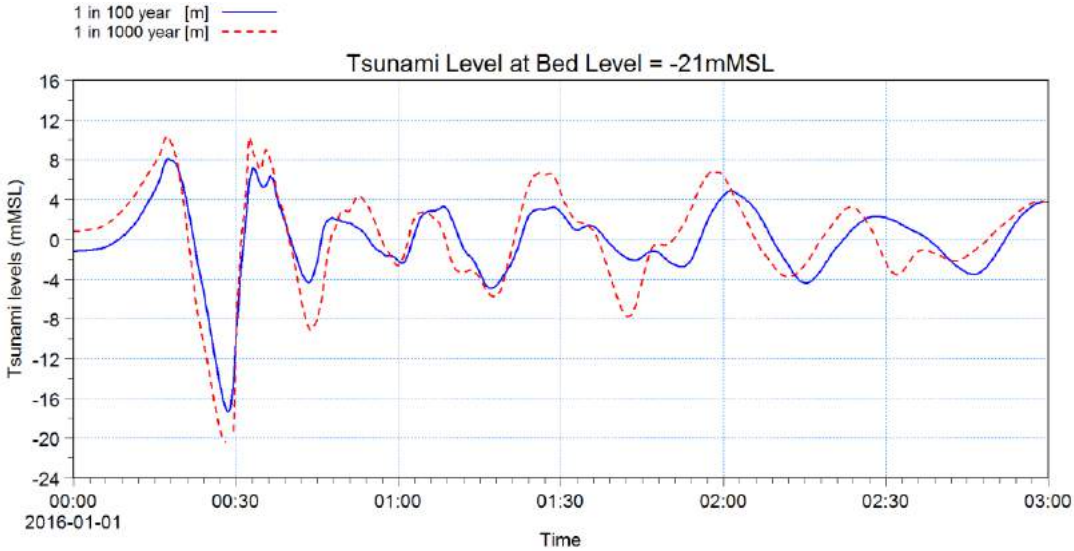

Fig. 9(f) Tsunami levels at seabed level of -21mMSL

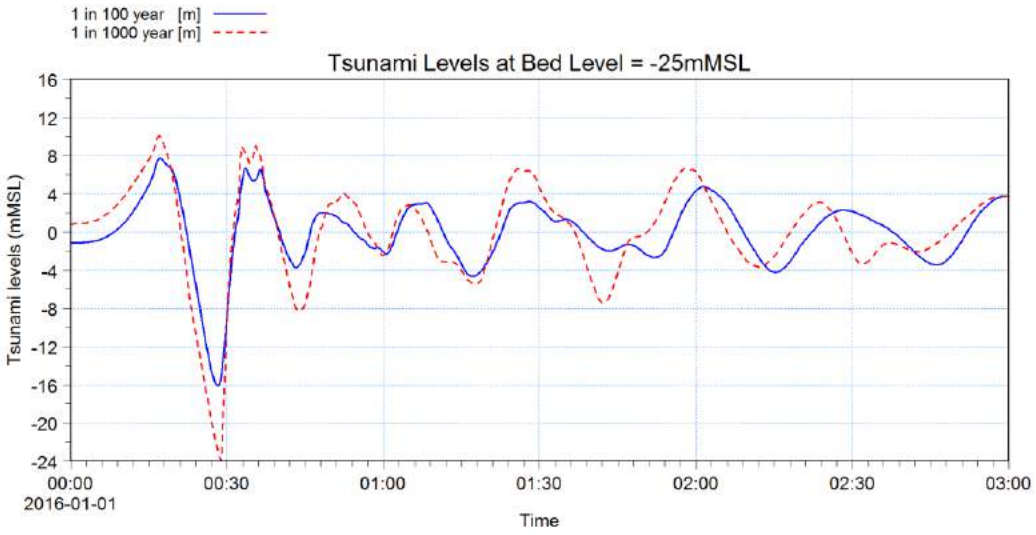

Fig. 9(g) Tsunami levels at seabed level of -25mMSL

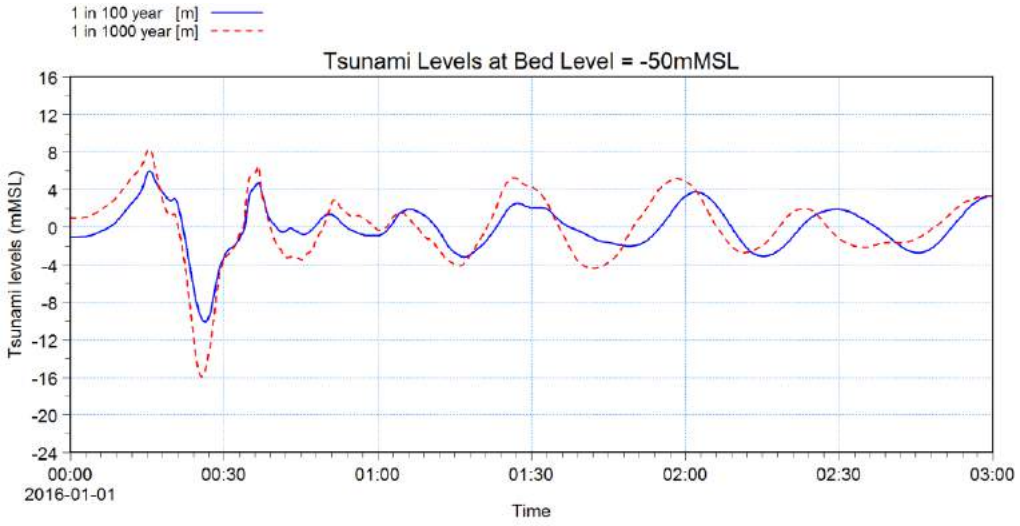

Fig. 9(h) Tsunami levels at seabed level of -50mMSL

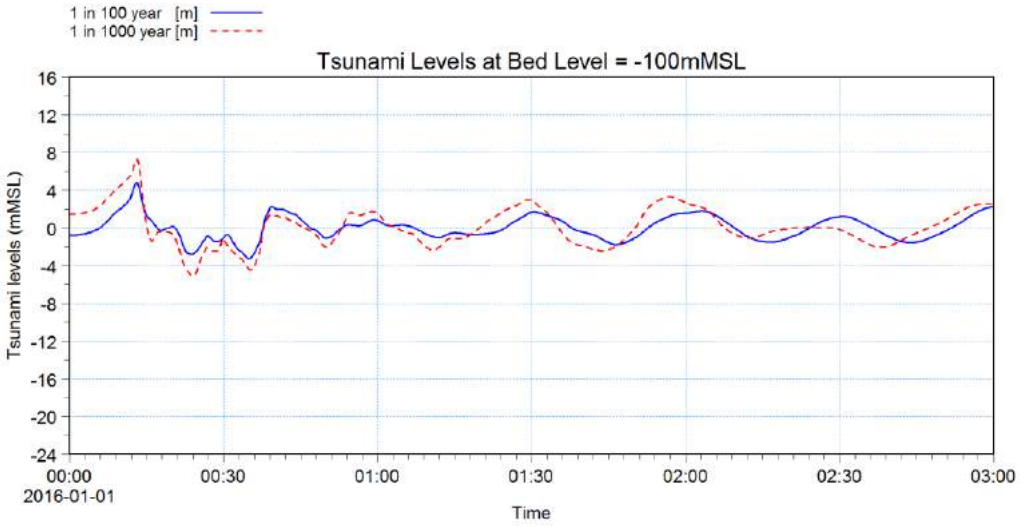

Fig. 9(i) Tsunami levels at seabed level of -100mMSL

Fig. 9 Tsunami levels at various water depths

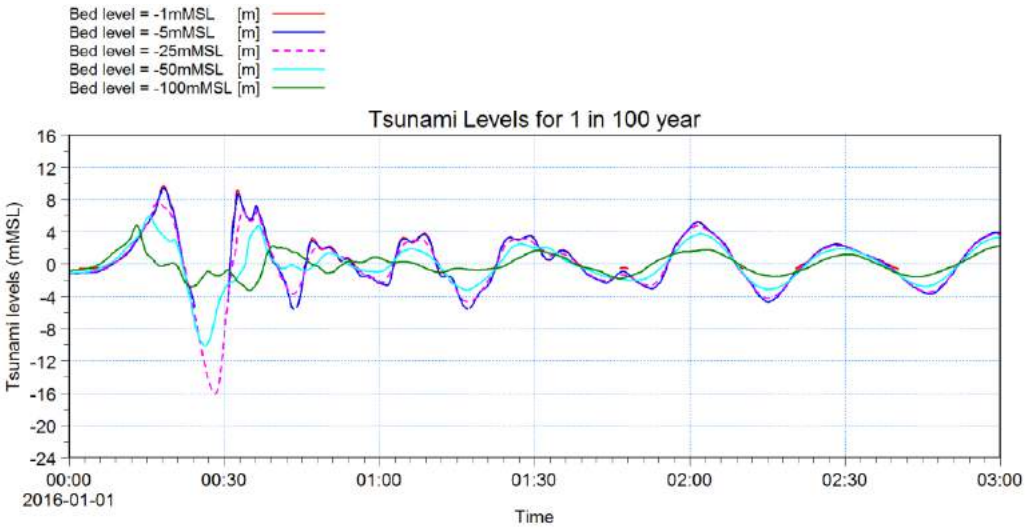

Fig. 10 Tsunami levels comparison at various water depths for Run 1 (1 in 100 year)

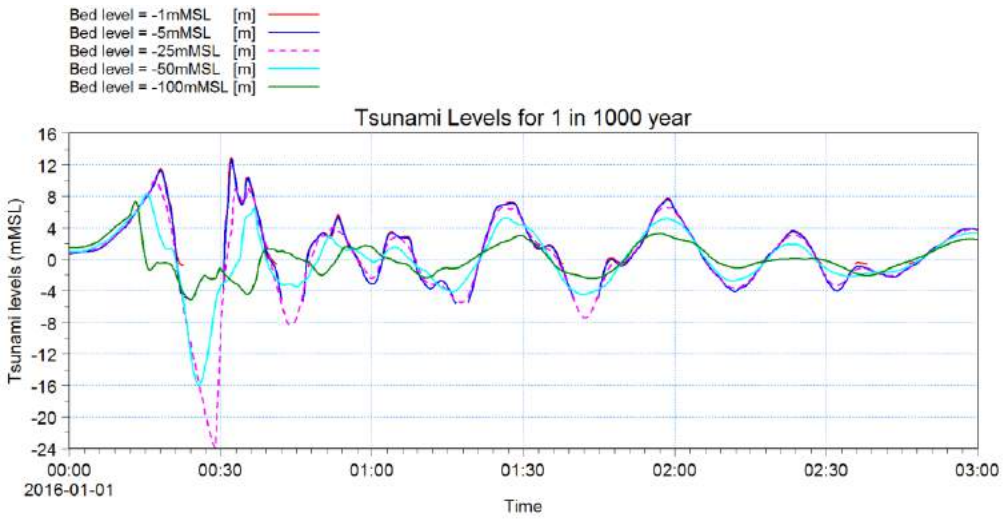

Fig. 11 Tsunami levels comparison at various water depths for Run 2 (1 in 1000 year)

6.9.4. Impact of water depths on maximum tsunami levels

Maximum tsunami levels were extracted from the model results at various water depths. Table 8 summarises the maximum tsunami levels at various water depths. The highest maximum tsunami levels were found at the shallowest bed level (i.e. at -1mMSL) and these are +9.7mMSL for Run 1 (1 in 100 year) and +12.9mMSL for Run 2 (1 in 1000 year).

Table -8 Maximum tsunami levels at various water depths

Bed levels (mMSL)	Maximum Tsunami Levels (+mMSL)	
	1 in 100 year (Run 1)	1 in 1000 year (Run 2)
-1	9.7	12.9
-3	9.6	12.8
-5	9.5	12.6
-12	9.0	12.3
-16	8.5	11.5
-21	8.1	10.5
-25	7.7	10.0
-50	6.0	8.4
-100	4.8	7.3

The maximum tsunami levels for 1 in 100 years and 1 in 1000 years conditions as provided in Table 8 were plotted in Figure 12 for ease of comparison. Consistently higher tsunami levels were found for the 1 in 1000 year condition as expected.

A relatively higher tsunami level was found at shallower waters as shown in Table 8 and Figure 12. The higher tsunami levels at shallower waters were due to shoaling effects as expected.

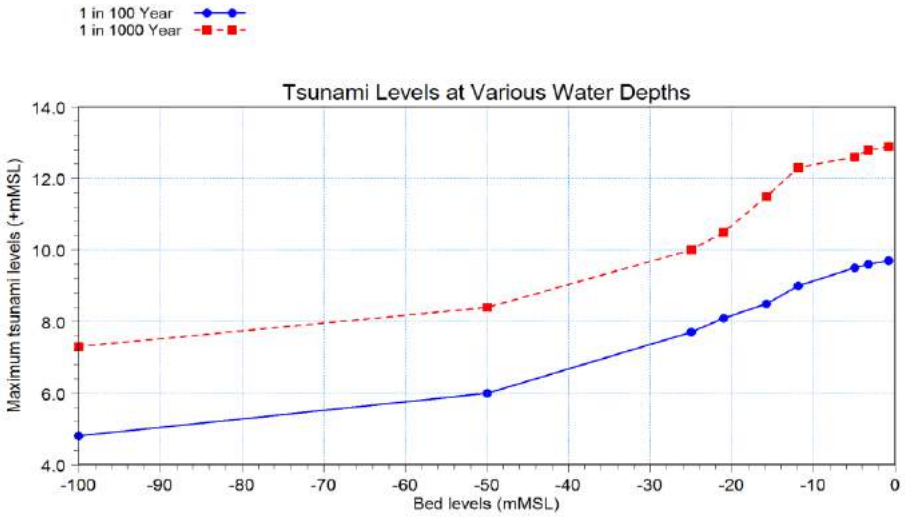

Fig. 12 Impact of water depths on maximum tsunami levels

6.9.5. Computed tsunami current velocities

Maximum current velocities were extracted from the model results over the entire domain as shown in Figures 13 and 14 for 1 in 100 years and 1 in 1000 years conditions respectively. The currents are resultant and depth-averaged. Stronger currents were found along the coastlines and inside the bays.

Model results were also extracted at various water depths. Figure 15 shows the current velocities at seabed level of -16mMSL. The highest current velocity was found after 30 minutes.

Table 9 summarises the maximum current velocities at various water depths. The highest maximum velocity was found to be 6.5m/s at seabed level of -16mMSL for the 1 in 100 year condition and 10.3m/s at seabed level of -12mMSL for the 1 in 1000 year condition.

Maximum tsunami currents for 1 in 100 years and 1 in 1000 years conditions as provided in Table 9 were plotted in Figure 16 for ease of comparison. A consistent higher tsunami current was found for the 1 in 1000 year condition as expected.

Table -9 Summary of the maximum resultant current velocities at various water depths

Bed levels (mMSL)	Maximum Resultant Current Speeds (m/s)	
	1 in 100 year (Run 1)	1 in 1000 year (Run 2)
-1	4.3	6.9
-3	4.7	8.2
-5	5.1	8.7
-12	6.2	10.3
-16	6.5	10.2
-21	6.4	9.8
-25	6.1	9.2
-50	4.0	5.5
-100	1.3	2.2

6.10. Discussions on Tsunami Model Results

Based on expectations, tsunami will intensify in bays, harbours and river mouths. Accordingly, higher tsunami levels and currents were found in bays compared to those in the open coasts.

The tsunami levels and velocities are found to be higher at shallower waters due to shoaling effects.

Because the earthquake return period investigations is not directly related to the earthquake location, the earthquake sources applied in this paper were assumed to be located at a particular location along the known fault line. Therefore, the model results should be considered to represent conservative values for this location. The tsunami levels, currents and run-up levels at this location will be smaller if the earthquake sources are located further away (north or south).

7. RUN-UP LEVEL CALCULATIONS

7.1. The Run-up Model and Approach

For the purpose of this tsunami wave run-up calculation, the AMAZON software was used. AMAZON is a high-resolution wave overtopping model developed by HaskoningDHV UK Ltd and the Manchester Metropolitan University [5]. It is a finite volume model of 2nd order upwind scheme and can use irregular, structured and boundary-fitted mesh. The model solves the shallow water equations of wave propagation and run-up providing time-series changes in water levels and depth-averaged velocities using random waves as a boundary condition. It takes into account the of wave

diffraction, refraction, reflection, wave breaking and other shallow water effects.
The AMAZON model requires input of a cross-shore profile, still water level and a time-series of tsunami wave heights.

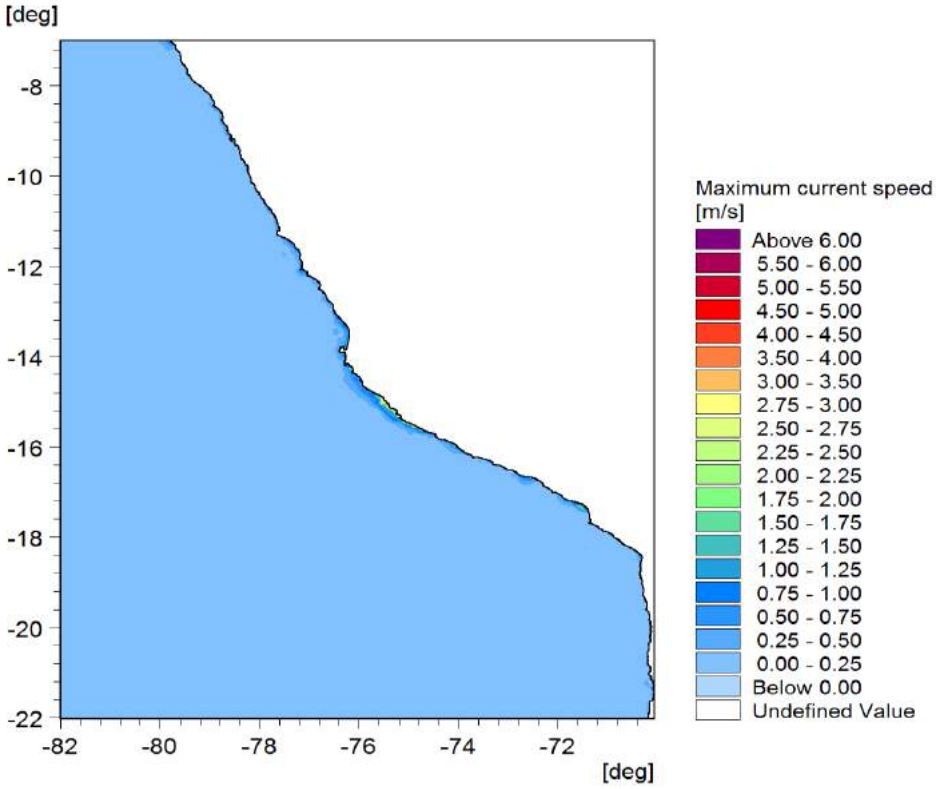

Fig. 13 Maximum tsunami currents for Run 1 (1 in 100 year)

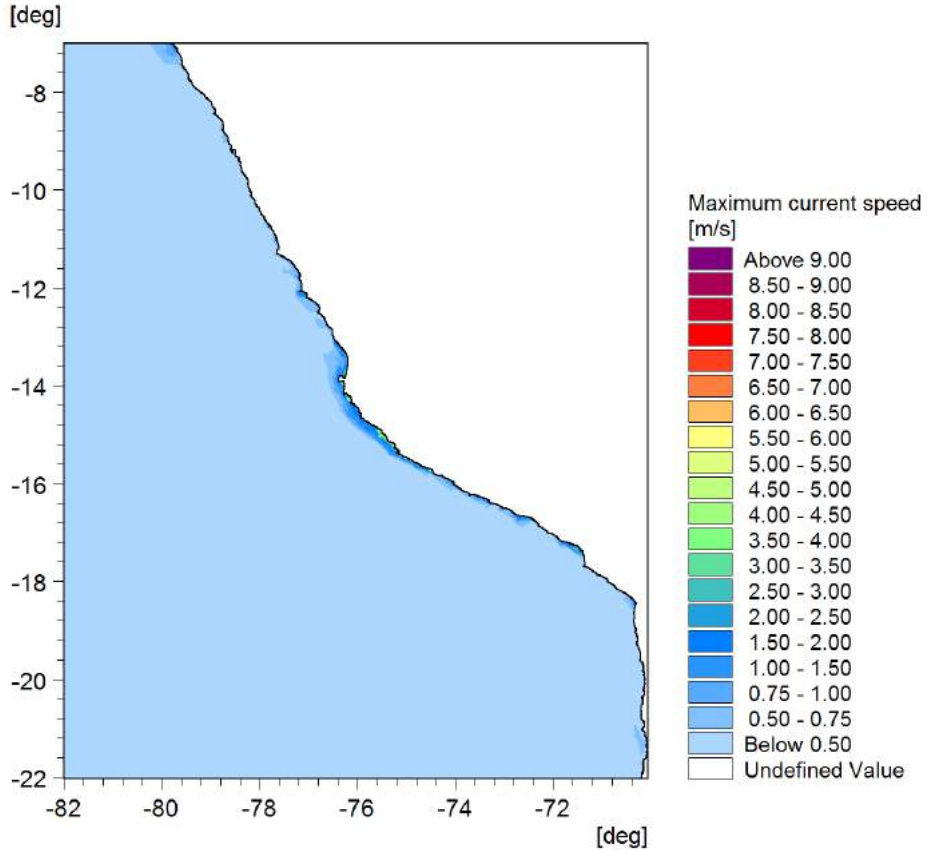

Fig. 14 Maximum tsunami currents for Run 2 (1 in 1000 year)

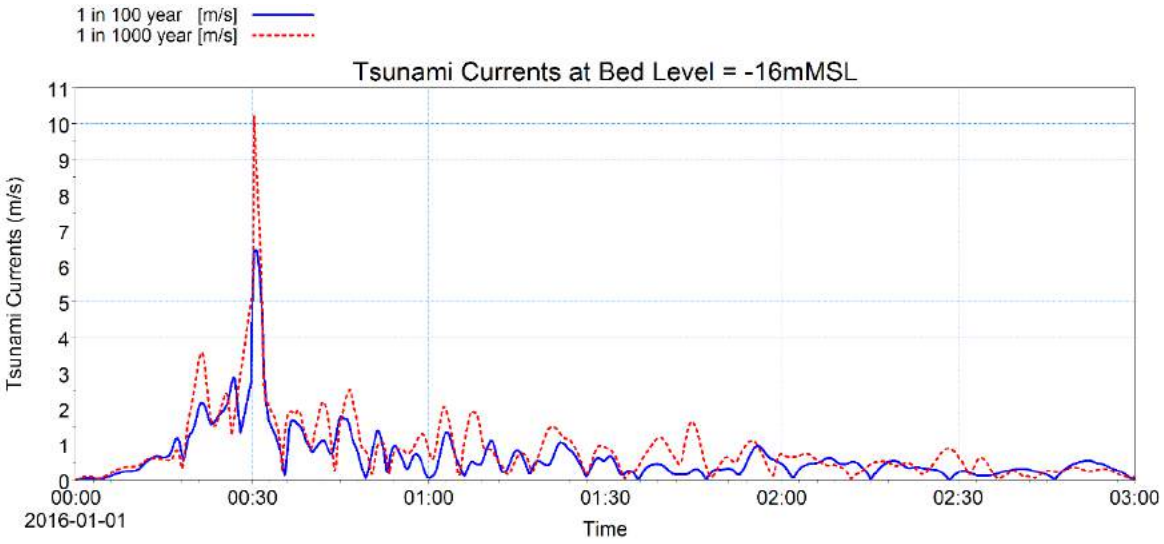

Fig. 15 Resultant tsunami current velocities at bed level -16mMSL

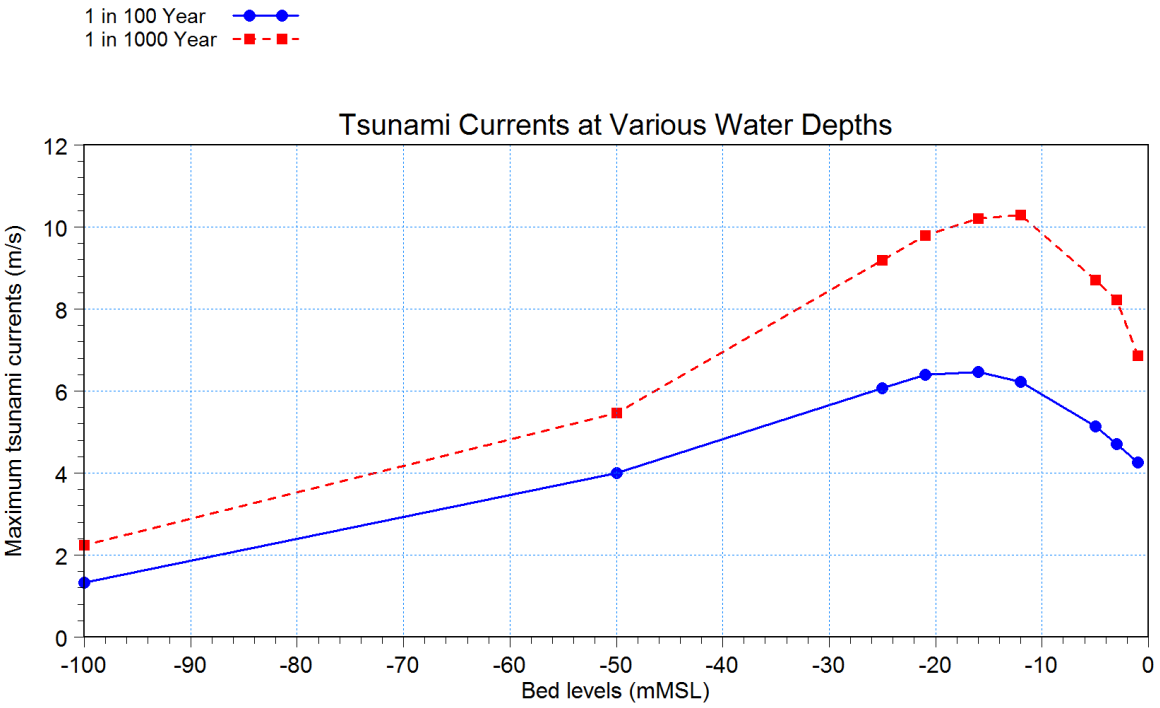

Fig. 16 Impact of water depths on tsunami currents

7.2. Run-up Model Setup

The cross-shore profile was extended up to approximately 3km offshore from the site location (up to -50m MSL bed level). Two return period events were considered, 1 in 100 years and 1 in 1000 years events, as in the tsunami modelling approach. Highest Astronomical Tide (HAT) of +0.67mMSL was used as the still water level. The model was driven by the tsunami waves as shown in Figure 9(h) extracted from the tsunami model at the first (offshore) point of the profile. A series of output points along the profile was selected to ensure the highest run-up point could be determined and used to derive the tsunami run-up level.

7.3. Run-up Model Validation

The findings from the International Tsunami Survey Team [19] was reported by [8] that the 2001 tsunami generated a maximum run-up of 7m at Camana.

The observed run-up from the 15 August 2007 tsunami caused by an earthquake of magnitude M_w 8.0 centred off the coast of central Peru was reported by [9]. The tsunami generated a locally focused run-up height of up to 10m.

Based on the data presented above, a good overall agreement was found in the magnitude of maximum run-up levels between previous studies and the results from the present study (as in Table 10). It should be noted that tsunami run-up level varies from location to location depending on slope of the profile.

7.4. Run-up Results

The results of the tsunami run-up simulations are presented in Table 10.

Table -10 Summary of the tsunami run-up levels

Return periods (year)	Run-up Levels (+mMSL)
100	14.9
1000	19.5

7.5. Discussion on Run-up Results

It should be noted that tsunami run-up level varies from location to location. Run-up over a steep slope is much higher than that over a mild slope. A concave profile would yield higher run-up than a linear or convex profile. A steep slope leads to higher run-up values than elsewhere along a coastline. Furthermore, run-up will be intensified in bays, harbours or river mouths.

The earthquake sources applied in this paper were assumed to be located in a particular location along the known fault line. Therefore, the model results should be considered to represent conservative values for that location. The tsunami run-up levels will be smaller if the earthquake sources are located further away (north or south).

8. SUMMARY AND FINDINGS

A tsunami risk assessment was carried out to identify the most critical tsunamigenic earthquake for the region. Return period conditions of earthquake magnitude (M_w) was determined for 1 in 100 year and 1 in 1000 year conditions.

Initial tsunami levels were generated using the Delft DashBoard developed by Deltares. Numerical modelling of tsunami propagation was undertaken using the MIKE21 Flow Model developed by DHI. A regional tidal hydrodynamic model was developed by RHDHV to drive the tsunami model. Tsunami model simulations were carried out for 1 in 100 years and 1 in 1000 years conditions. Run-up levels were calculated from tsunami levels using the AMAZON Model.

The maximum tsunami levels, resultant currents and run-up levels at the site are provided in Tables 8, 9 and 10 respectively.

The findings from the study may be summarised as follows:

a) The study suggests that the region is significantly affected by the tsunamis.
b) The maximum initial tsunami levels for 1 in 100 year and 1 in 1000 year conditions were +5.8mMSL and +8.6mMSL respectively.
c) The simulations indicate that it will take about 18 minutes for the peak tsunami wave generated on the fault line to reach the coastline.
d) It will take about 30 minutes for the peak tsunami currents to be generated.
e) Maximum tsunami levels and velocities are higher at shallower waters due to shoaling effects.
f) The maximum run-up levels for 1 in 100 year and 1 in 1000 year conditions were +14.9mMSL and +19.5mMSL respectively.

Acknowledgements

The author would like to thank Royal HaskoningDHV (an independent, international engineering and project management consultancy company, www.royalhaskoningdhv.com) for giving permission to publish this paper.

References

[1]. PIANC, *Mitigation of Tsunami Disasters in Ports*, The World Association for Waterborne Transport Infrastructure, Permanent International Association of Navigation Congresses (PIANC), Maritime Navigation Commission Report Number 112, 2010, http://www.pianc.org.
[2]. Wikipedia, Tsunami, Web. https://en.wikipedia.org/wiki/Tsunami, 2017.
[3]. Deltares, Delft DashBoard, P.O. Box 177, 2600 MH Delft, the Netherlands, 2016.
[4]. DHI, MIKE21 Flow Model User Guide, Agern Alle 5, DK-2970 Hosholm, Denmark, 2016.
[5]. K Hu, CG Mingham and DM Causon, Numerical Simulation of Wave Overtopping of Coastal Structures by Solving NLSW Equations, *Coastal Engineering*, 2000, Vol. 41, pages 433-465.
[6]. EA Kulikov, AB Rabinovich and RE Thomson, Long-term Tsunami Forecasting, *Oceanology*, 2005, 45(4), pages 488-499, Pleiades Publishing Inc.
[7]. P Belle, Great Earthquakes of Peru. Power Point presentation slides obtained from *http://web.gps.caltech.edu/~clay/PeruTrip/Talks/Philibosian_PeruEQs.pdf*, 2010.
[8]. EA Okal, JC Borrero and CE Synolakis, Evaluation of tsunami risk from regional earthquakes at Pisco, Peru, *Bulletin of the Seismological Society of America*, 2006, 96(5), pages 1634-1648, doi: 10.1785/0120050158.
[9]. HM Fritz, N Kalligeris JC Borrero, P Broncano and E Ortega, The 15 August 2007 Peru tsunami run-up observations and modelling, *Geophysical Research Letters*, 2008, Vol. 35, L10604, doi: 10.1029/2008GL033494.
[10]. E Mas, B Adriano, N Pulido, C Jimennez and S Koshimura, Simulations of Tsunami Inundation in Central Peru from Future Megathrust Earthquakes Scenarios, *Journal of Disaster Research*, 2014, 9(6), pages 961-967.

[11]. N Pulido, H Tavera, Z Aguilar, D Calderon, M Chlieh, T Sekiguchi, S Nakai and F Yamazaki, Mega-Earthquakes Rupture Scenarios and Strong Motion Simulations for Lima, Peru, *The International Symposium for CISMID 25th Anniversary on Technological Advances and Learned Lessons from last Great Earthquakes and Tsunamis in the World*, held in Lima (Peru), during 17-18 August 2012, Paper Number TS-6-2.

[12]. E Silgado, Recurrence of Tsunamis in the Western Coast of South America, *Mar. Geod., 1978*, 1(4), pages 347–354.

[13]. C-Map, JEPPESEN Commercial Marine, Hovlandsveien 52, Egersund, Postal Code 4370, Norway, *http://www.c-map.no*, www.jeppesen.com, 2014.

[14]. Y Okada, Surface deformation due to shear and tensile faults in a half-space. *Bulletin of the Seismological Society of America*, 1985, 75(4), pages 1135-1154.

[15]. NH Pedersen, PS Rasch and T Sato, Modelling of the Asian tsunami off the coast of Northern Sumatra, Tsunami Paper_v5.doc/NHP et al., 31-03-2005 prepared by DHI and Alpha Hydraulic Engineering Consultant Co. Ltd., Sapporo, Japan. *www.mikepoweredbydhi.com*/upload/dhisoftwarearchive/.../TsunamiPaper_v5.pdf.

[16]. SA Luger and RL Harris, Modelling tsunamis generated by earthquakes and submarine slumps using MIKE21, *Prestedge Retief Dresner Wijnberg*, Cape Town, South Africa. www.dhigroup.com/upload/publications/mike21/Luger_2010.pdf.

[17]. MM Hasan, SMM Rahman and U Mahamud, Numerical modelling for the propagation of tsunami wave and corresponding inundation, *IOSR Journal of Mechanical and Civil Engineering (IOSR-JMCE)*, 2015, 12(2), pages 55-62. iosrjournals.org/iosr-jmce/papers/vol12-issue2/Version-4/I01245562.pdf.

[18]. MA Sarker and AJ Sleigh, Cyclone and Tsunami Hazards in the Arabian Sea – A Numerical Modelling Case Study by Royal Haskoning DHV, *Journal of Shipping and Ocean Engineering*, 2015, 5(5), pages 242-254, DOI 10.17265/2159-5879/2015.05.003, USA.

[19]. EA Okal, L Dengler, S Araya, JC Borrero, B Gomer, S Koshimura, G Laos, D Olcese, M Ortiz, M Swensson, VV Titov and F Vegas, A field survey of the Camana, Peru tsunami of June 23, 2001, *Seism. Res. Lett.* 73, 2002, pages 904-917.